Effects of Size and Surface Treatment on Fatigue Life of Fused Filament Fabrication Manufactured Acrylonitrile Butadiene Styrene Parts

Jianchi Huang
Department of Engineering Technology and Industrial Distribution;
Department of Mechanical Engineering,
Texas A&M University,
College Station, TX 77843
e-mail: jianchi1994@tamu.edu

Eduardo Miscles
Department of Mechanical Engineering,
University of New Mexico,
Albuquerque, NM 87131
e-mail: emiscles@unm.edu

Tara Mellor
Department of Mechanical and Aerospace Engineering,
University of California,
Los Angeles, CA 90095
e-mail: taramellor@ucla.edu

Chao Ma
Department of Engineering Technology and Industrial Distribution;
Department of Mechanical Engineering,
Texas A&M University,
College Station, TX 77843
e-mail: cma@tamu.edu

Mathew Kuttolamadom
Department of Engineering Technology and Industrial Distribution,
Texas A&M University,
College Station, TX 77843
e-mail: mathew@tamu.edu

Jyhwen Wang[1]
Department of Engineering Technology and Industrial Distribution;
Department of Mechanical Engineering,
Texas A&M University,
College Station, TX 77843
e-mail: jwang@tamu.edu

An experimental study was conducted to study the effects of geometric size and surface treatment on the fatigue life of fused filament fabrication (FFF) manufactured acrylonitrile butadiene styrene (ABS) parts. Moore rotating-beam fatigue tests were conducted with four different levels of loadings to obtain the S–N curves. Two different sizes (control size and large size) and three different surface treatment methods (as-printed, acetone-treated, and sandpaper polished) were studied. The larger specimens had significantly decreased fatigue life because of a larger volume, and hence a greater probability of defects for crack initiation and propagation, as compared with the control specimen. The acetone-treated specimen had a smooth surface. Its fatigue life, however, decreased significantly because the acetone treatment caused internal damage that weakened the specimen and was reported for the first time. The sandpaper polished specimen also had a smooth surface, but its effect on the fatigue life was insignificant because the extruded filament direction on the specimen surface was parallel to the loading direction. The present results lead to a better understanding of the effects of geometric size and surface treatment on the fatigue performance of FFF specimens. The study also provides important insights for the design of part size and surface treatment of three-dimensional (3D) printed plastic components for fatigue loading end-use applications.
[DOI: 10.1115/1.4050178]

Keywords: additive manufacturing, fatigue life

1 Introduction

Various additive manufacturing (AM) processes have been used to make quick and sufficiently accurate prototypes for design validation. Fused filament fabrication (FFF), a material extrusion additive process, is one of the most common methods of additive manufacturing due to its affordability, production speed, and versatility. The ability to create complex three-dimensional (3D) geometry with a single setup and minimal human interaction has caused a shift in its use from rapid prototyping to rapid manufacturing [1]. Making end-use components with FFF means that the mechanical performance of the manufactured thermoplastics parts must be understood. A significant portion of AM parts for end-use is currently in metals, but additive manufacturing of polymeric materials is becoming more prevalent throughout the industry [1]. There is mature knowledge of the static properties of FFF manufactured thermoplastics [2], but little exists on their fatigue behavior. Hence, experimentation of thermoplastic AM parts to better understand their fatigue performance is warranted.

Failure caused by cyclic loading below yielding is a fatigue phenomenon, and this can occur in metals and polymers by crack initiation and propagation [1]. If components are manufactured for cyclic loading end-use, their fatigue life should be considered during the design process.

The effect of geometric size is a critical concern for end-use components. The size factor is well-studied both experimentally and analytically for other materials such as metals, alloys, and concrete [3–10]. However, a study of size factors on the fatigue life of 3D printed plastics has not been reported, as listed in Table 1. A general conclusion is that larger parts consist of more material and are more susceptible to defects and failure than smaller parts. The larger number of defects can provide more sites for crack initiation and propagation, and thus result in a shorter fatigue life. On the contrary, the size effect for alloys is more material sensitive, so the size effect could be insignificant or significant depending on the alloying materials [5,9]. Hence, the size effect on the fatigue life of 3D printed plastics drew the authors' attention.

Surface treatment is also important to improve the performance of end-use components. Some researchers studied the improvement of the surface appearance of FFF specimens with chemical treatment like acetone and found that acetone could cause re-flow of acrylonitrile butadiene styrene (ABS) materials resulting in the formation of a thin smooth layer on the specimen surface [11–15], as listed in Table 1. Neff et al. [11] found that the effect of acetone treatment was not significant on the ultimate tensile strength (UTS), but some sharp defects could be observed on the treated surface, which could give rise to stress concentration. Gao et al. [12] found that the acetone treatment could also decease the ultimate tensile strength slightly. Mu et al. [13] found that the tensile strength decreased as the acetone treatment time increased and the

[1]Corresponding author.
Manuscript received October 8, 2020; final manuscript received February 6, 2021; published online March 29, 2021. Assoc. Editor: Jingjing Li.

Table 1 Comparison of different works of fatigue

Material	Studied printing orientation effect on tensile strength	Studied surface treatment effect on tensile strength	Studied printing orientation effect on fatigue life	Studied surface treatment effect on fatigue life	Studied size effect on fatigue life	Reference
ABS	Yes	Yes	No	No	No	[11] [12] [13]
ABS	No	No	No	No	No	[14]
Ultem 9085	No	No	Yes	Yes	No	[15]
CFRP ABS/TPU	Yes	No	No	No	No	[16] [17] [18]
ABS PLA	Yes	No	Yes	No	No	[19] [23] [25] [28] [29]
ABS	No	No	Yes	No	No	[20] [22]
PLA ABS	Yes	No	No	No	No	[21] [24] [26] [27]
ABS	No	No	No	Yes	Yes	This work

weight of the specimen increased as the acetone treatment time increased. Singh et al. [14] did some parametric studies to optimize the surface vapor smoothing process. Fischer and Schöppner [15] found that the effect of chloroform treatment on the tension–tension fatigue life of Ultem 9085 was not significant. However, there is no result reported regarding the effect of acetone treatment for cyclic tension–compression loading as in the rotating-beam fatigue testing. Besides, the previous focus was on the improvement of the surface but what happened to the chemical-penetrated cross section was not investigated nor did the possible effect on the fatigue life. Moreover, mechanical treatment methods such as sandpaper polishing can also improve the surface finish, but there is a lack of published results on the effect of mechanically polished surface finish on the fatigue life of FFF specimens.

For end-use components, printing parameters are also critical but are well-studied by researchers. The effects of printing orientation and raster orientation on the fatigue life of AM parts have been well-studied by researchers, as listed in Table 1. A 45 deg flat printing orientation was found to be able to give the best fatigue strength and tensile strength with different plastics and specimen geometries such as (1) ABS flat dog bones [16–19,23,25,26,28,29], (2) ABS cuboids with a notch [22,24], (3) ABS cylindrical specimens [20], (4) PLA flat dog bones [21], and (5) polycarbonate rectangle specimens [27]. However, most of the aforementioned research focused on the parametric study of printing processes.

The objective of this research is to investigate the effects of geometric size and surface treatment on the fatigue life of ABS specimens manufactured by FFF. In the present work, the specimens prepared by FFF were characterized based on fully reversed stress ratio ($R = -1$) for the first time. This stress ratio is similar to that of a rotating shaft application. The *S–N* diagrams were plotted, and the fractographic images of the failed cross section were analyzed. The results and discussions also provided insights into the design of the geometry/size and surface treatment of 3D printed plastic components for fatigue loading end-use applications.

2 Experimental Methods

2.1 Printing Setup. A LulzBot TAZ 6 desktop 3D printer with a 0.5 mm diameter extrusion nozzle was used for this study. The 3 mm diameter commercial black ABS filament (Chromastrand Labs, CO) was selected as base feedstock material for printing. From tensile tests of flat dog bone specimens printed with this ABS, the UTS of this ABS was 40 MPa. The pre-set high-detail mode with ABS printing settings was used to define the printing temperatures for the nozzle and heat plate during the printing process. A 0.3 mm layer height was used based on the recommendation of the printer which was also beneficial to reduce the printing time. The printing orientation was 0 deg (the angle between the longitude direction of the specimen and the *X*-axis defined by ISO/ASTM 52921:2013(E)) with a zig-zag 100% infill density to achieve ±45 deg raster lines. This printing orientation was selected, as it was reported to give the highest fatigue strength [16–29]. Support structures were generated and used to help increase the printing quality. During the printing process, the printer was insulated by an enclosure made with acrylic board and aluminum foil to obtain a better printing quality. The building direction is indicated in Fig. 1. After the printing, support structures were removed from all the specimens without damaging the specimen surfaces.

2.2 Specimen Sizes. Two different sizes of cylindrical dog-bone-shaped specimens were printed and used for the fatigue test to investigate the effect of geometric size. As shown in Fig. 1, the

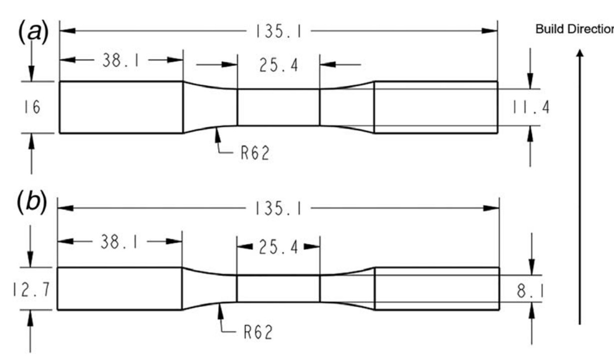

Fig. 1 Dimensions (in mm) of specimens: (a) large specimen and (b) control specimen

total lengths of the two specimens were the same, at 135.1 mm, and the neck lengths were both at 25.4 mm. The neck diameters are different. An $8.1^{+0.2}_{-0.0}$ mm neck diameter was used as the baseline/control size. Instead of an ISO standard size, an $11.4^{+0.2}_{-0.0}$ mm neck diameter was used for the large size specimen to accommodate the fixture on the rotating-beam fatigue testing machine. As a result, the cross-sectional area ratio of the large specimen to the control specimen was approximately 2. The diameters at both ends were 12.7 mm for the control specimen and 16.0 mm for the large size specimen, respectively. For both specimens, an arc with a 62 mm radius connected the neck section to the two ends.

2.3 Surface Treatments. To study the effect of surface treatment on the fatigue life of FFF manufactured parts, the as-printed surface with control size was used as the baseline. Within the same control size, acetone-treated surfaces and sandpaper polished surfaces were obtained and tested to investigate the effect of surface treatment.

For acetone treatment, a large piece of aluminum foil was placed into a large stainless-steel container to cover the bottom and side surfaces. Then, three pieces of the paper towel were placed on the foil to overlap the same area and 50 ml acetone was sprayed evenly on the paper towel. After that, flat supports made with aluminum foils were placed in the container and printed specimens were placed horizontally on the supports. Hence, specimens were elevated within an acetone vapor environment. Another piece of foil was placed in the container as an inner cover, and the container was closed with a stainless-steel lid. The specimens were treated at room temperature with no external heating, and three specimens were treated at each time. After 3 h, the specimens were taken out from the container and were left out for resting naturally in the air at room temperature. The specimens were available for testing after 24 h. For sandpaper polishing, the specimens were mounted on a spindle (with both end supported) rotating at 2000 rpm. A piece of 200-grid sandpaper was used to polish the surface of the neck section of the rotating specimen for 2 min. Then, the process was repeated with a 340-grid sandpaper for 1 min to complete the polishing process. The reduction in the neck diameter after treatment was measured. The tolerance was controlled within the range between 0.2 mm and 0.25 mm. Hence, the diameter of the neck of the sandpaper polished sample was $8.1^{+0.00}_{-0.25}$ mm.

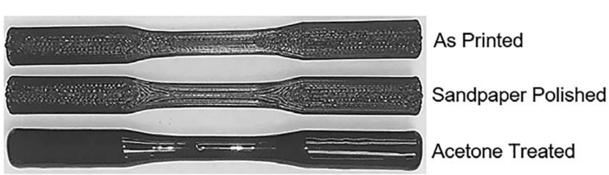

Fig. 2 Different treated surfaces from top to bottom: as-printed, sandpaper polished, and acetone treated

Figures 2 and 3 show the different treated surfaces with different magnifications. The extruded cylindrical filament can be observed on the as-printed surface. On the surface of the sandpaper polished specimen, the outline of the cylindrical extruded filament can still be observed, but the waviness of the surface was reduced compared with that of the as-printed specimen. Among the three different surfaces, the acetone-treated one looks smooth and reflective and differs dramatically from the other two. Roughness was not measured because extruded filaments and grooves were dominant in the longitudinal direction and characterizing the circumference with waviness did not serve a useful purpose.

2.4 Rotating-Beam Fatigue Test. A custom Moore-type rotating-beam fatigue test machine was used to conduct the fatigue tests. As shown in Fig. 4, the specimen was held between the two rigid collets. The collet was connected to a rigid mount with bearing supports, so the collets could rotate freely on the mount and pivot about the mounting shaft. Weights were hung below both collets to provide the designated loading. One of the collets was connected to a motor by a flexible coupling. During testing, the motor was set to rotate at 2000 rpm. A rotating shaft counter was attached to one of the shafts to record the number of revolutions. When a specimen failed, one of the collets pivoting down would contact a sensor to stop the counter and switch off the motor.

To obtain the *S–N* curves and study the fatigue characteristics of various specimens, different loading conditions resulting in different loading stresses were needed. Based on the dimensions of the specimens and the testing apparatus, the four-point bending model was used to calculate the stresses. According to the discrete weights available for loading, the stresses were set at 40, 50, 62, and 72 MPa. Within each loading stress, the test was repeated three times to ensure the repeatability.

3 Results

3.1 The Effect of Size on Fatigue Life. Figure 5 shows the *S–N* diagram of the size effect. It is shown that the fatigue life decreases with increased specimen size, and the difference is significant at about one order of magnitude. The reason for the reduced fatigue life due to the size effect is known for other materials such as metals, alloys, and concrete [3–10]. Larger specimen size can contain more defects for crack initiation and propagation during the fatigue test. In practical applications, a *size factor* can be established to quantitatively predict the decrease in fatigue life for larger specimens. According to the results, the stress that the control specimen can take at a 10,000 fatigue-life-cycle is about 78 MPa, while that of the large specimen at the same loading cycles is only about 39 MPa, which indicates an approximately 50% fatigue strength. Based on the literatures on endurance limit and with the control size as the reference, the size factor forspecimen with larger cross

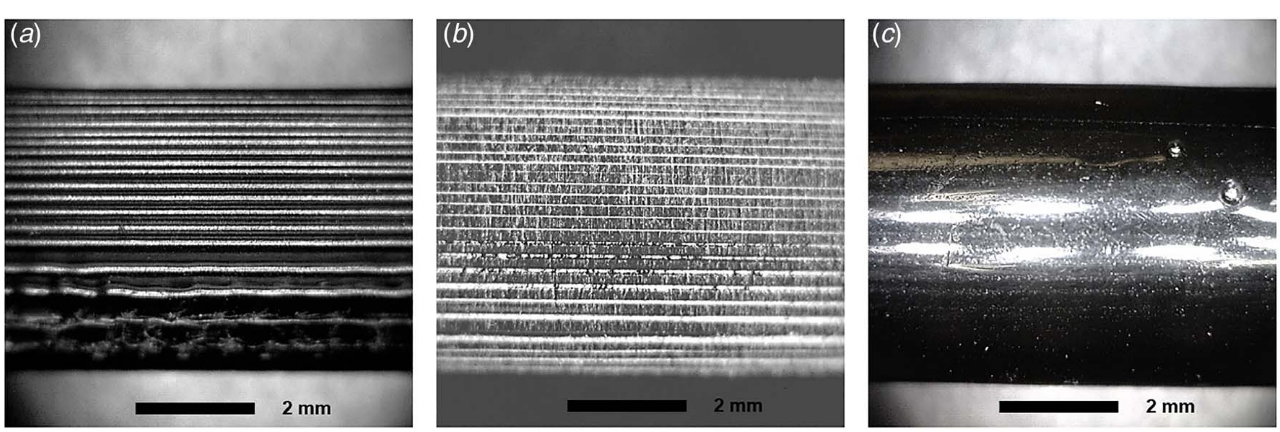

Fig. 3 Different treated surfaces with higher magnification: (*a*) as-printed, (*b*) sandpaper polished, and (*c*) acetone treated

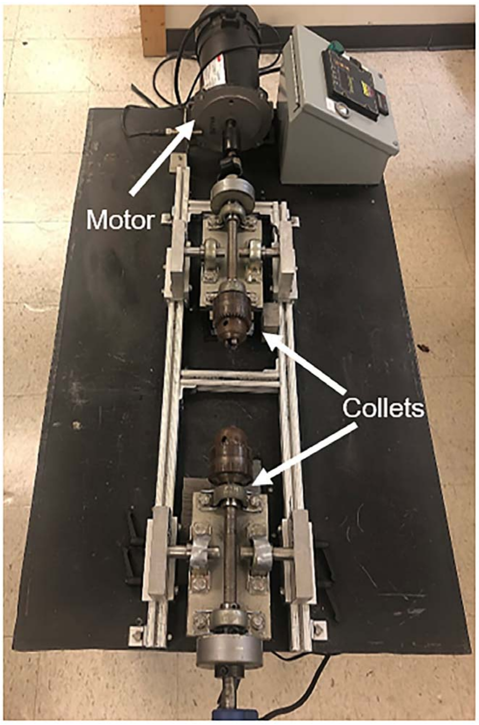

Fig. 4 The custom Moore-type rotating-beam fatigue test machine used for fatigue life characterization

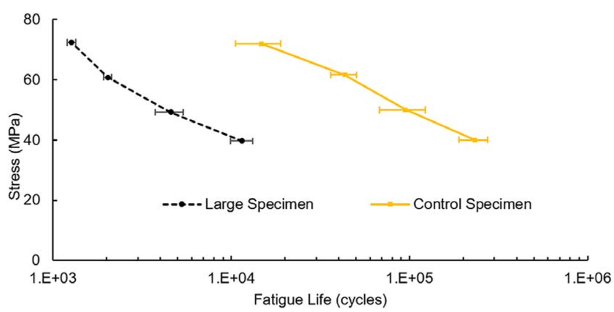

Fig. 5 *S–N* diagram of the size effect

section is 0.96 (96%) for metal specimens [3–10]. This study demonstrates a significantly lower fatigue strength of 50% for the FFF AM parts. A more detailed discussion on the size effect based on the observed fracture surfaces is presented in Sec. 4.1.

3.2 The Effect of Surface Treatment on Fatigue Life. For specimens with smooth surface, such as those from acetone and sandpaper treatments, the fatigue life, in theory, should increase with better surface finish. This is because finer surface finish can reduce stress concentration for crack initiation and propagation from the surface. Figure 6 shows the *S–N* diagram of the surface treatment effect. It can be observed that with sandpaper polishing, the fatigue life remains approximately the same as the control specimen. On the other hand, the fatigue life of the acetone-treated specimen, with excellent surface finish, is significantly reduced by about one order of magnitude. Neff et al. [11] conducted tensile tests of flat dog bone acetone-treated specimens and reported that the tensile strength was slightly reduced due to changes in the size and shape of the pores. In the present work, a more drastic change of the internal structure of the specimens is observed. Based on fractographic images, a detailed discussion of the effect of surface treatment on fatigue life is presented in Sec. 4.2.

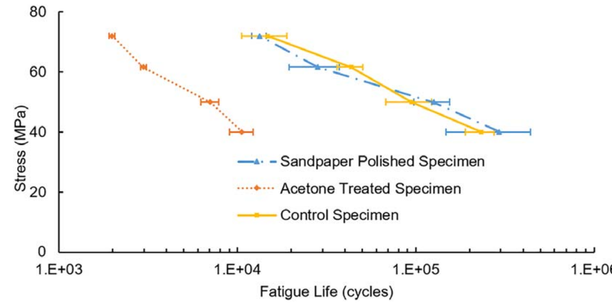

Fig. 6 *S–N* diagram of the surface treatment effect

As can be observed from the error bars, Figs. 5 and 6 show good repeatability of the conducted experiments. It is known that the quantitative fatigue life depends heavily on the specifics of the specimens, such as surface finish, stress type, geometric size, and other factors. The present study suggests that the surface and size effects should not be overlooked as their quantitative values are quite different from those presented in previous studies.

4 Discussion

4.1 The Effect of Size on Fatigue Failure. Figure 7 shows the fracture surfaces of the control specimens at different loading stresses. On all the fracture surfaces, a white region can be observed. The white region is the instantaneous fracture zone (indicated by the white rectangle frame), indicating the loading stress is greater than the UTS at fracture. The whitening of the region could be crazing and due to the alignment of ABS molecules in tensile loading [30]. It is noted that as the loading stress increases, the stress reaches the UTS faster after crack initiation and propagation, which results in an increased area of the white region. On the opposite side of the white region, fatigue striation markings (indicated by the white solid arrows) are clearly observed in Figs. 7(*a*)–7(*c*). These markings are due to crack growth and arrest. As the specimen is subjected to repeated, reversed bending stress, it can be identified that the origin of the fatigue crack is at the edge, on the concave side of the markings. As shown in the figures, the spacing of the markings is progressively wider toward the direction of crack propagation. The wider spacing reflects the increased stress at reduced cross-sectional area during the test. Also observed from the figures is that while the loading stress increases, the area with fatigue striation decreases because of higher crack propagation speed. When the loading stress is as high as 72 MPa, as shown in Fig. 7(*d*), no striation mark is visible because the cracks propagate rapidly, which results in a short fatigue life that coincides with the fatigue testing results. In addition to the striation markings, ratchet marks in the form of loose extruded filaments (indicated by the white dashed arrows) are present around the circumference. This indicates the intersection and connection of fatigue fractures propagating from multiple origins at the initial stage of fatigue testing [30].

The fracture surfaces of large size specimens are shown in Fig. 8. Similar to that of the control specimens, cracks also initiate at some points on the circumference and quickly propagate through the cross section. An apparent difference is that, at the same loading stress, the fraction of the white region of the large size specimens is greater than that of the control specimens. In the white region, a large number of pores can be observed, which are more than those in the control specimens. The large number of defects within the large specimens may cause increased stress concentration sites and accelerate crack propagation. Besides, no fatigue striation marking is observed for large specimens, a sign of short fatigue life, even at the lowest loading stress of 40 MPa.

4.2 The Effect of Surface Treatment on Fatigue Failure. Figure 9 shows the cross-section surfaces of (Fig. 9(*a*)) as-printed

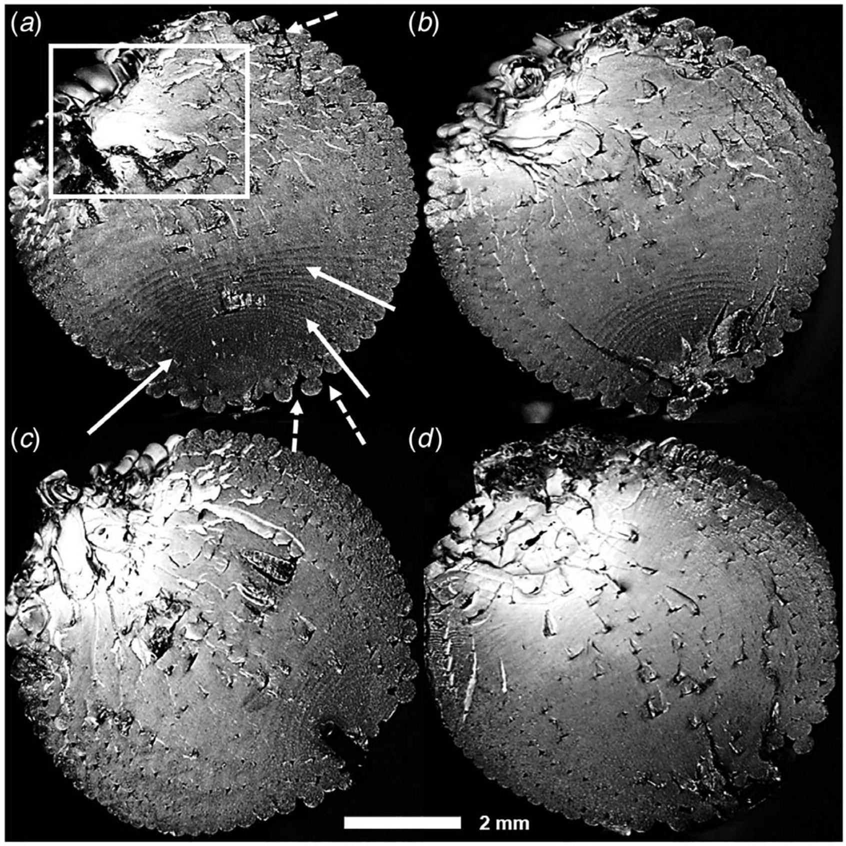

Fig. 7 Fracture surfaces of control specimens at (*a*) 40 MPa, (*b*) 50 MPa, (*c*) 62 MPa, and (*d*) 72 MPa loading stress

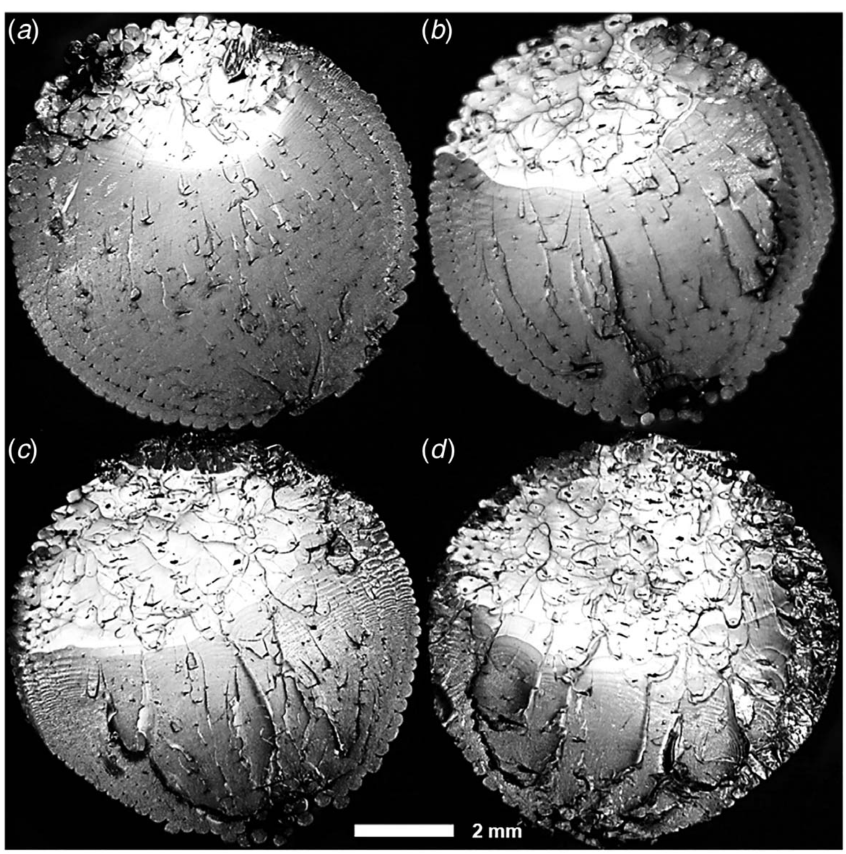

Fig. 8 Fracture surfaces of large size specimens at (*a*) 40 MPa, (*b*) 50 MPa, (*c*) 62 MPa, and (*d*) 72 MPa loading stress

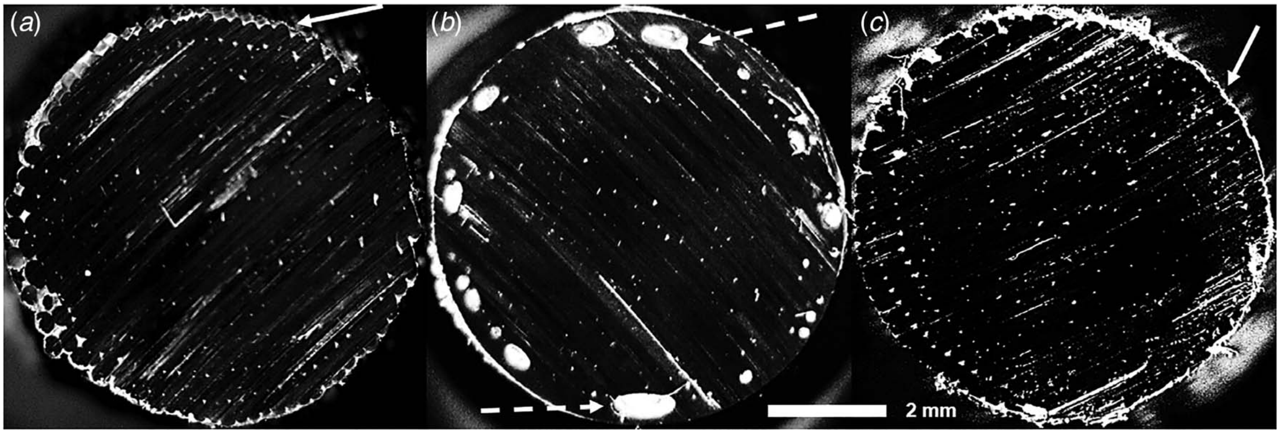

Fig. 9 Cross section surface of specimens before fatigue testing: (*a*) as-printed specimen, (*b*) acetone-treated specimen, and (*c*) sandpaper polished specimen

specimen, (Fig. 9(*b*)) acetone-treated specimen, and (Fig. 9(*c*)) sandpaper polished specimen before fatigue testing. The scratches on each cross section are the machine marks caused by the sectioning process. The cross section of the acetone-treated specimen looks drastically different from that of the control specimen. The circumference is very smooth with no sign of extruded filaments. It appears that the ABS material can flow and rearrange its form due to surface tension. Another interesting observation is that there are some large pores (indicated by dashed white arrows) formed in an annual ring just inside of the circumference. It is known that ABS does not react chemically with acetone. The weight of a specimen increases immediately after treatment, but gradually decreases to its initial weight [11]. Mu et al. [13] found that the initial weight increase corresponds to the treatment time, and acetone treatment has a more severe effect on the geometry, weight, and UTS of the specimen than pure ethyl acetate treatment. Thus, the large pores could be a

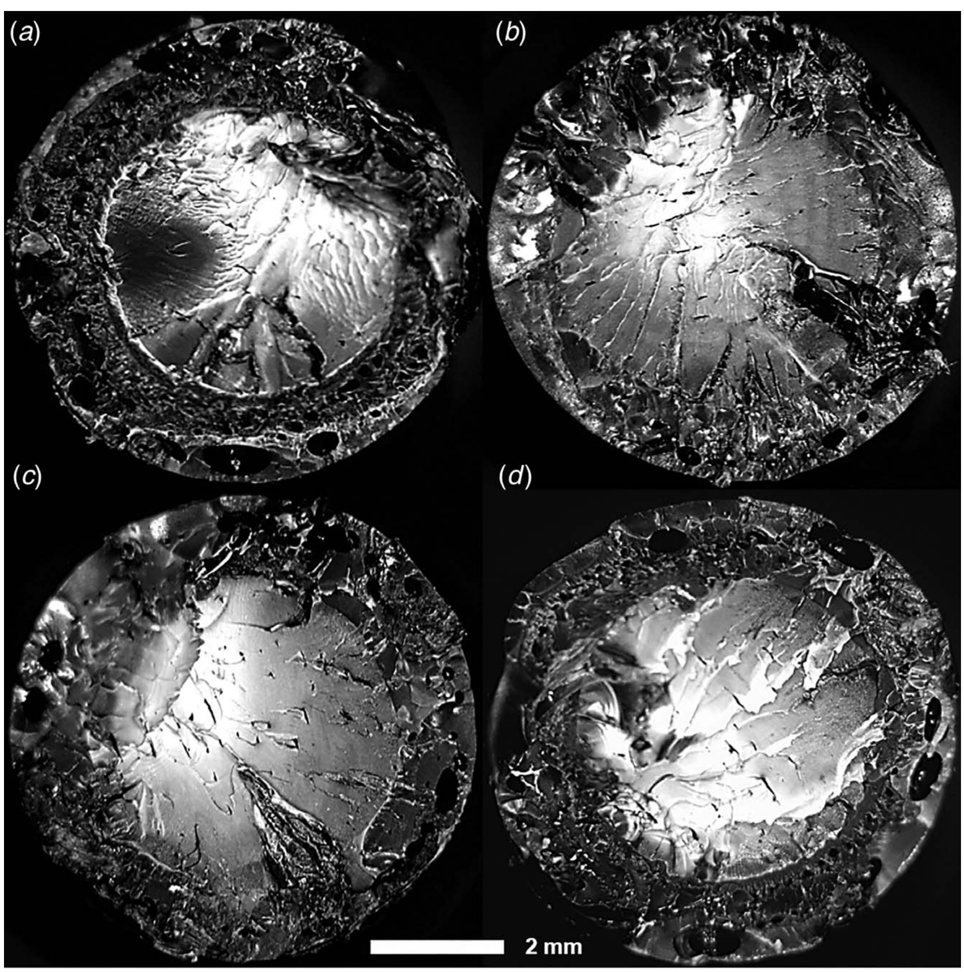

Fig. 10 Fracture surfaces of acetone-treated specimens at (*a*) 40 MPa, (*b*) 50 MPa, (*c*) 62 MPa, and (*d*) 72 MPa loading stress

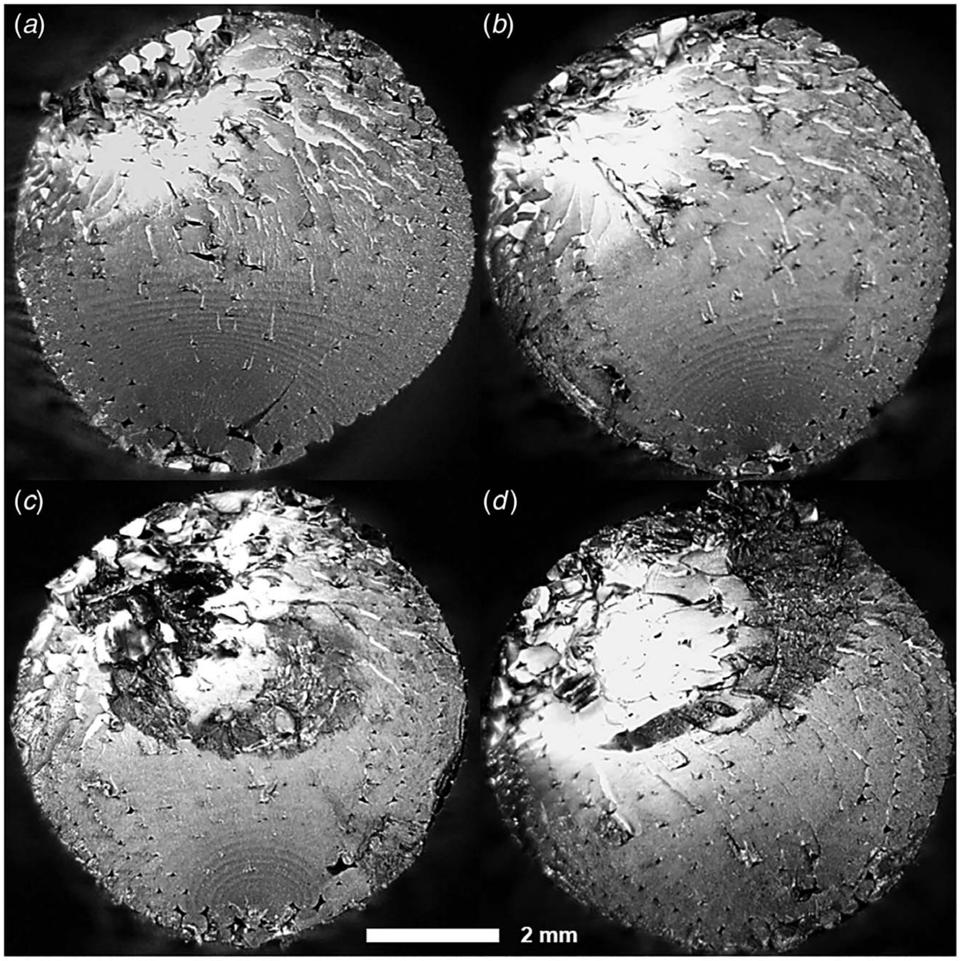

Fig. 11 Fracture surfaces of sandpaper treated specimens at (*a*) 40 MPa, (*b*) 50 MPa, (*c*) 62 MPa, and (*d*) 72 MPa loading stress

result of fusion of preexisting small pores in the cross section and the re-flow of ABS could also turn open pores into closed pores during the treatment. From Fig. 10(*c*), it can be observed that the sandpaper polished specimen has a cross section similar to that of the control specimen, except that the ridges and grooves at the circumference (indicated by solid white arrows) are partially removed due to polishing.

As described in Sec. 3.2 and contrary to the previously known surface treatment effect on fatigue life, the acetone-treated specimen with fine surface finish fared much worse than the control specimen in the fatigue testing. Fischer and Schöppner [15] found the effect of chloroform treatment on the tension–tension fatigue life of Ultem 9085 was not significant. The difference between their results and the results of this study could be due to the difference in specimen geometry and loading condition. Besides, the difference in printed materials and surface treatment chemicals can also lead to difference in the results. Figure 10 shows the fracture surfaces of acetone-treated specimens at different loading stresses. A shell-like annual ring in the outer region can be observed. The rings correspond to that of the specimen shown in Fig. 9(*b*). The rings/shells in all specimens have the same thickness and contain large pores, which indicate that the porous shells are created by acetone penetration. In the core region of the cross section, the fracture surface is similar to that of the control specimens. The area of the white region increases as the loading stress increases. However, there is no fatigue striation marking observed. From the test data, it can be noted that the improvement of surface finish after acetone treatment is not enough to compensate for the internal damage that is also associated with the same treatment. It appears the weak shells change the uniformity of the ABS specimen and fracture first during fatigue testing. The damage reduces the effective diameter of the cross section and significantly increases the loading stress at the core. The condition leads to rapid crack initiation and propagation, an indication of short fatigue life that agrees with the fatigue testing results. In Ref. [15], it is not clear whether the same shell structures appear at the cross section of the treated flat dog bone specimen and the shell structures could have a more significant effect on the fatigue life of the specimen with a bending loading condition than that of a tensile–tensile loading condition.

Figure 11 shows the fracture surfaces of sandpaper polished specimens with different loading stresses. Compared with Fig. 7, there is no significant difference between the sandpaper polished specimen and the control specimen at the same loading stress. As loading stress increases, the changes in the corresponding white region and striation region are almost the same. The observations agree with the fatigue test results, where the fatigue life of the

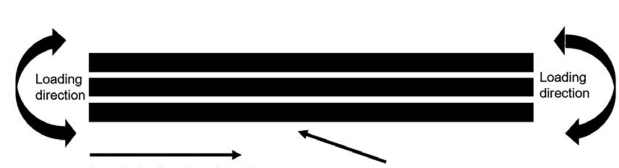

Fig. 12 Schematics of extruded filament direction on the specimen surface and loading direction

printed specimens is not affected by sandpaper treatment. The reason could lie in the relationship between the extruded filament direction and the loading direction, as shown in Fig. 12. During 3D printing, although the infill of the specimen is filled by crisscross rasters layer-by-layer, the perimeter of the layer is printed separately as a continuous contour. As a result, the outer surface consists of extruded filaments align with the longitudinal direction of the specimen. In the rotating-beam four-point bending test, the direction of tension–compression stress is also in the longitudinal direction. For sandpaper treatment, since the surface change is mostly in the circumferential direction, the fatigue life remains almost unchanged after surface refinement with sandpaper polishing.

5 Conclusions

While there is a large knowledge base in fatigue of the metallic part made from traditional processes, fatigue of the polymer-based AM part has not been well investigated. In this research, the effects of geometric size and surface treatment on the fatigue life of ABS specimens manufactured by FFF were studied. The experiments were conducted with specimens obtained from the desktop FFF printer. While the printer used in this study is not an industrial-grade printer, the fatigue life (hundreds of thousands cycles) of the printed parts is acceptable for end-use when the loading stress is low. The investigation on the effects of geometric size of the part and surface treatment provides a qualitative insight that is applicable to the application of better quality parts printed from industrial-grade printers. For the effect of geometric size, a larger size is found to decrease the fatigue life significantly, because a larger size specimen has more material volume, and hence greater probability for more defects, leading to more stress concentration and crack initiation sites (similar to the fatigue behavior of parts made from other manufacturing processes). For the tested specimen sizes, the large size would result in a 96% fatigue strength when compared with the control size for typically metal specimens. In contrast, the fatigue strength of the large size is only 50% of the control size for FFF specimens in this study. While the fatigue limit is not investigated in the present work, it is clear that a new correction factor is required to account for the effect of part size on the fatigue performance. For the effect of surface treatment, the treatment that results in a smooth surface finish cannot always ensure an increase in fatigue life. Acetone treatment decreases the fatigue life significantly because it creates a weak shell structure with high porosity just below the smooth surface. This observation answered the question of why a better surface finish can lead to a worse fatigue performance. In the present study, sandpaper polishing does not affect the fatigue life much because the extruded filament direction on the specimen surface is aligned with the bending stress direction. It can be concluded that, in this case, filament/printing direction on the outer surface is a more dominant factor than surface modification for fatigue performance. The results from the current study suggest that further investigation in fatigue life prediction is required for designers to adopt FFF for fatigue loading end-use applications.

Acknowledgment

This material is based upon work partially supported by the National Science Foundation under Grant No. 1659856. Any opinions, findings, and conclusions or recommendations expressed in this material are those of the authors and do not necessarily reflect the views of the National Science Foundation.

Conflict of Interest

There are no conflicts of interest.

Data Availability Statement

The datasets generated and supporting the findings of this article are obtainable from the corresponding author upon reasonable request. The authors attest that all data for this study are included in the paper.

References

[1] Safai, L., Cuellar, J. S., Smit, G., and Zadpoor, A. A., 2019, "A Review of the Fatigue Behavior of 3D Printed Polymers," Addit. Manuf., **28**, pp. 87–97.

[2] Cuan-Urquizo, E., Barocio, E., Tejada-Ortigoza, V., Pipes, R. B., Rodriguez, C. A., and Roman-Flores, A., 2019, "Characterization of the Mechanical Properties of FFF Structures and Materials: A Review on the Experimental, Computational and Theoretical Approaches," Materials, **12**(6), 895.

[3] Ai, Y., Zhu, S. P., Liao, D., Correia, J. A. F. O., Souto, C., De Jesus, A. M. P., and Keshtegar, B., 2019, "Probabilistic Modeling of Fatigue Life Distribution and Size Effect of Components With Random Defects," Int. J. Fatigue, **126**, pp. 165–173.

[4] Carpinteri, A., Spagnoli, A., and Vantadori, S., 2009, "Size Effect in S-N Curves: A Fractal Approach to Finite-Life Fatigue Strength," Int. J. Fatigue, **31**(5), pp. 927–933.

[5] El Khoukhi, D., Morel, F., Saintier, N., Bellett, D., Osmond, P., Le, V. D., and Adrien, J., 2019, "Experimental Investigation of the Size Effect in High Cycle Fatigue: Role of the Defect Population in Cast Aluminium Alloys," Int. J. Fatigue, **129**, p. 105222.

[6] Kloos, K. H., Buch, A., and Zankov, D., 1981, "Pure Geometrical Size Effect in Fatigue Tests With Constant Stress Amplitude and in Programme Tests," Materialwiss. Werkstofftech., **12**(2), pp. 40–50.

[7] Phillips, C. E., and Heywood, R. B., 1951, "The Size Effect in Fatigue of Plain and Notched Steel Specimens Loaded Under Reversed Direct Stress," Proc. Inst. Mech. Eng., Part E, **165**(1), pp. 113–124.

[8] Shirani, M., and Härkegård, G., 2011, "Fatigue Life Distribution and Size Effect in Ductile Cast Iron for Wind Turbine Components," Eng. Failure Anal., **18**(1), pp. 12–24.

[9] Zhu, S. P., Foletti, S., and Beretta, S., 2018, "Evaluation of Size Effect on Strain-Controlled Fatigue Behavior of a Quench and Tempered Rotor Steel: Experimental and Numerical Study," Mater. Sci. Eng., A, **735**, pp. 423–435.

[10] Zdenek, P. B., and Kangminh, X., 1991, "Size Effect in Fatigue Fracture of Concrete," ACI Mater. J., **88**(4), pp. 390–399.

[11] Neff, C., Trapuzzano, M., and Crane, N. B., 2018, "Impact of Vapor Polishing on Surface Quality and Mechanical Properties of Extruded ABS," Rapid Prototyp. J., **24**(2), pp. 501–508.

[12] Gao, H., Kaweesa, D. V., Moore, J., and Meisel, N. A., 2017, "Investigating the Impact of Acetone Vapor Smoothing on the Strength and Elongation of Printed ABS Parts," JOM, **69**(3), pp. 580–585.

[13] Mu, M., Ou, C. Y., Wang, J., and Liu, Y., 2020, "Surface Modification of Prototypes in Fused Filament Fabrication Using Chemical Vapour Smoothing," Addit. Manuf., **31**, p. 100972.

[14] Singh, R., Singh, S., Singh, I. P., Fabbrocino, F., and Fraternali, F., 2017, "Investigation for Surface Finish Improvement of FDM Parts by Vapor Smoothing Process," Composites, Part B, **111**, pp. 228–234.

[15] Fischer, M., and Schöppner, V., 2017, "Fatigue Behavior of FDM Parts Manufactured With Ultem 9085," JOM, **69**(3), pp. 563–568.

[16] Kim, J., and Kang, B. S., 2018, "Optimization of Design Process of Fused Filament Fabrication (FFF) 3D Printing," ASME Int. Mech. Eng. Congr. Expo. Proc., **2**, pp. 1–8.

[17] de León, A. S., Domínguez-Calvo, A., and Molina, S. I., 2019, "Materials With Enhanced Adhesive Properties Based on Acrylonitrile-Butadiene-Styrene (ABS)/ Thermoplastic Polyurethane (TPU) Blends for Fused Filament Fabrication (FFF)," Mater. Des., **182**, p. 108044.

[18] Mazzei Capote, G. A., Redmann, A., and Osswald, T. A., 2019, "Validating a Failure Surface Developed for ABS Fused Filament Fabrication Parts Through Complex Loading Experiments," J. Compos. Sci., **3**(2), 49.

[19] Frascio, M., Avalle, M., Monti, M., Rabbi, M. F., Chalivendra, V. B., and Li, D., 2019, "The Effect of Raster Orientation on the Static and Fatigue Properties of Filament Deposited ABS Polymer," ASME Int. Mech. Eng. Congr. Expo. Proc., **124**, pp. 1–16.

[20] Domingo-Espin, M., Travieso-Rodriguez, J. A., Jerez-Mesa, R., and Lluma-Fuentes, J., 2018, "Fatigue Performance of ABS Specimens Obtained by Fused Filament Fabrication," Materials, **11**(12), pp. 1–16.

[21] Rajpurohit, S. R., and Dave, H. K., 2018, "Impact of Process Parameters on Tensile Strength of Fused Deposition Modeling Printed Crisscross Polyactic Acid," Int. J. Mater. Met. Eng., **12**(2), pp. 52–57.

[22] Frascio, M., Avalle, M., and Monti, M., 2018, "Fatigue Strength of Plastics Components Made in Additive Manufacturing: First Experimental Results," Proc. Struct. Integr., **12**, pp. 32–43.

[23] Lee, J., and Huang, A., 2013, "Fatigue Analysis of FDM Materials," Rapid Prototyp. J., **19**(4), pp. 291–299.

[24] Rabbi, M. F., Chalivendra, V. B., and Li, D., 2019, "A Novel Approach to Increase Dynamic Fracture Toughness of Additively Manufactured Polymer," Exp. Mech., **59**(6), pp. 899–911.

[25] Afrose, M. F., Masood, S. H., Iovenitti, P., Nikzad, M., and Sbarski, I., 2016, "Effects of Part Build Orientations on Fatigue Behaviour of FDM-Processed PLA Material," Prog. Addit. Manuf., **1**(1–2), pp. 21–28.
[26] Zhang, H., Cai, L., Golub, M., Zhang, Y., Yang, X., Schlarman, K., and Zhang, J., 2018, "Tensile, Creep, and Fatigue Behaviors of 3D-Printed Acrylonitrile Butadiene Styrene," J. Mater. Eng. Perform., **27**(1), pp. 57–62.
[27] Puigoriol-Forcada, J. M., Alsina, A., Salazar-Martín, A. G., Gomez-Gras, G., and Pérez, M. A., 2018, "Flexural Fatigue Properties of Polycarbonate Fused-Deposition Modelling Specimens," Mater. Des., **155**, pp. 414–421.
[28] Ziemian, S., Okwara, M., and Ziemian, C. W., 2015, "Tensile and Fatigue Behavior of Layered Acrylonitrile Butadiene Styrene," Rapid Prototyp. J., **21**(3), pp. 270–278.
[29] Ziemian, C. W., Ziemian, R. D., and Haile K, V., 2016, "Characterization of Stiffness Degradation Caused by Fatigue Damage of Additive Manufactured Parts," Mater. Des., **109**, pp. 209–218.
[30] Hayes, M. D., Edwards, D. B., and Shah, A. R., 2015, "Fractography Basics," *Fractography in Failure Analysis of Polymers*, S. Ebnesajjad, ed., Elsevier, New York, pp. 48–92.